Proceedings World Geothermal Congress 2020+1
Reykjavik, Iceland, April - October 2021

Pressure Interference Tests at the Wasabizawa Geothermal Field, Akita Prefecture, Japan

Hiroaki Asai[1], Shigetaka Nakanishi[1], Shigeo Tezuka[1], Chitoshi Akasaka[1], Kenji Sasaki[1], Kengo Takizawa[1], Takashi Kaneko[2], and Shuji Ajima[3]

[1]Electric Power Development Co. Ltd. (J-Power), 15-1, Ginza 6-chome, Chuo-ku, Tokyo, 104-8165 Japan
[2]Mitsubishi Gas Chemical Company, Inc. (MGC), Tokyo, Japan
[3]Yuzawa Geothermal Power Corporation (YGP), Akita, Japan

Hiroaki_Asai@jpower.co.jp

Keywords: Wasabizawa, pressure transient test, pressure interference test, fractured reservoir, steam cap

ABSTRACT

The Wasabizawa geothermal field is located in Akita prefecture, northeastern Honshu. Commercial operation of the Wasabizawa geothermal power station (46.199 MWe) began in 2019. The subsurface stratigraphy consists of a sequence of volcanic rocks overlying naturally-fractured granitic basement rocks. The geothermal reservoir is hosted by the naturally-fractured granitic rocks. Fault systems striking along NW-SE, NE-SW and E-W trends are inferred by geophysical surveys (gravity survey and MT & CSAMT surveys). Targeting these estimated fault zones, a total of 11 production and reinjection wells, in addition to five existing exploration wells which will be converted to production and injection wells, were drilled during construction of the power station, and an extensive heterogeneity of fracture distribution in the granitic basement rock was observed. To delineate the permeability structure for the area, numerous pressure transient tests were performed during short term production from and injection into newly drilled wells. Analyses of pressure interference data indicate that the reservoir has a modest transmissivity of 3-17 Darcy-m. Reservoir temperature and pressure profiles suggest that two phase regions (steam cap) may exist just below the cap rock in eastern part of the field where depth of reservoir top is relatively shallow. Relatively large value for the storage parameter ϕch ($1\text{-}3 \times 10^{-7}$ m/Pa) obtained by pressure interference analysis in eastern production wellfield also suggests that steam cap exists at the top of the reservoir and affects the pressure transient response.

1. INTRODUCTION

An extensive exploration program consisting of geological, geochemical, and geophysical surveys, core hole drilling, well drilling, and pressure transient testing has been carried out at the Wasabizawa geothermal field, located in Akita prefecture, northeastern Honshu (see Figure 1). The exploration program involved two geothermal promotion surveys supported by the New Energy and Industrial Technology Organization (NEDO); i.e. for the Wasabizawa area and the adjacent Akinomiya area as shown in Figure 1. Over 30 exploratory wells have been drilled in the area so far, and the reservoir character is relatively well delineated. J-Power, Mitsubishi Materials Corporation (MMC) and Mitsubishi Gas Chemical Company, Inc. (MGC) jointly established the Yuzawa Geothermal Power Corporation (YGP) in 2010 to manage the geothermal resource and to accelerate geothermal exploration for both areas in a unified manner. YGP planned a 46.199MWe double-flash plant, and the construction works including drilling of new production and injection wells commenced in May 2015.

Stable temperature profiles in representative wells, shown in Figure 2, exhibit conduction-dominated behavior in a low-permeability shallow caprock layer through which heat flows from the underlying geothermal reservoir upward into the shallow groundwater system. The caprock appears to extend down to depths corresponding to between +200 m ASL and -200 m ASL, depending on the horizontal location, below which the convection-dominated reservoir is found at temperatures between 280°C and 290°C. Nakanishi et al. (2020) describe a conceptual model of the field as shown in Figure 3, which provided technical basis for planning the power station. The geothermal reservoir is hosted by naturally fractured granitic rocks, and the fracture network is developed beneath relatively impermeable cap rock layer. Fault systems striking along NW-SE, NE-SW and E-W trends are inferred by geophysical surveys (gravity survey and MT & CSAMT surveys). Based on the conceptual model, and considering the surface topography and location of existing exploratory wells, the location of production well pads and reinjection well pads were planned to be set about 2 km apart from each other. We set three production well pads (WA, WB at highest elevation of +930 m ASL, and WC) and two reinjection well pads (AA and AB at lowest elevation of +620 m ASL). Planned production zone to the east and injection zone to the west are also shown in Figure 3. A total of 11 production and reinjection wells, in addition to five existing exploration wells which will be converted to production and injection wells, were drilled targeting inferred fault zones, and an extensive heterogeneity of fracture distribution in the granitic basement rock was observed. Locations of newly drilled wells as well as exiting wells are shown in Figure 4. Correlation of pressure with equivalent feed point elevation is shown in Figure 5. The figure shows that almost all wells in the area including newly drilled production and injection wells are in good pressure communication with each other, except two wells (YO-8 and AY-5) located to the west; the feedpoint pressures of these two wells are about 1 MPa lower than those of other wells relative to the same elevation. The feedpoint pressures of the latter wells suggest that the reservoir is isolated from these wells and nearby Akinomiya hot spring area by a relatively impermeable zone, as shown in Figure 3. Comparing saturation temperature profile corresponding to the reservoir pressure with stable temperature profiles in wells, it is likely that a two-phase region (steam cap) exists just below the cap rock in eastern part of the field where elevation of the reservoir top is relatively high.

YGP performed numerous pressure transient tests during injection and production tests, including single well injection tests, pressure buildup tests and interference tests during short term production tests of newly drilled production wells. This paper describes the analyses of those pressure interference tests as well as single well tests to delineate the permeability structure of the field.

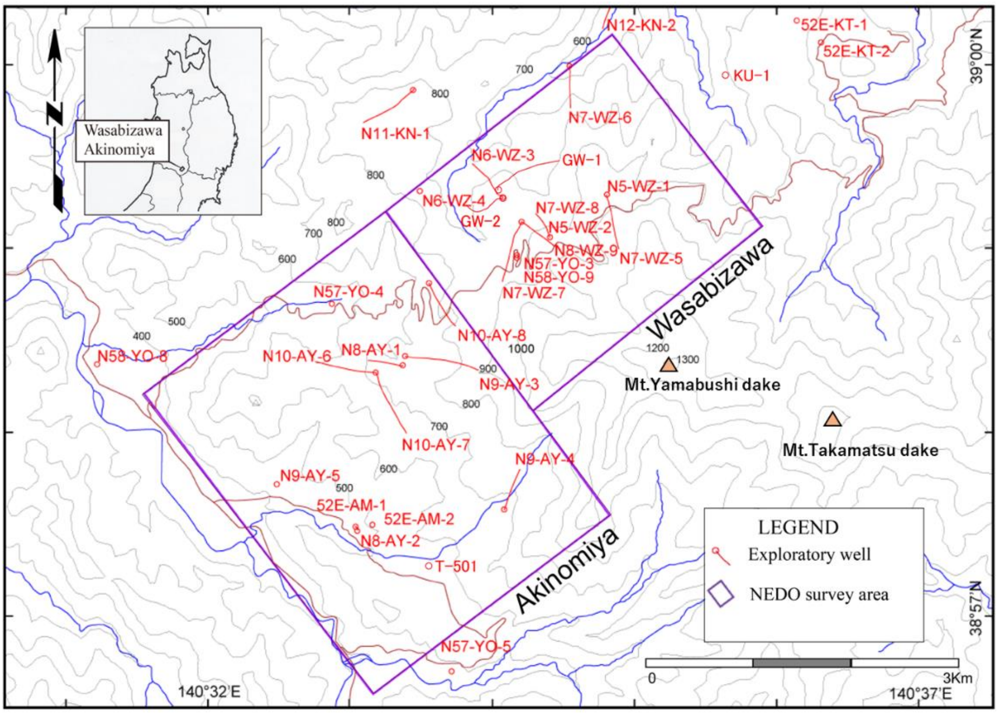

Figure 1: Exploratory well location in the Wasabizawa geothermal field. Black: ground surface elevation contours (0.1 kilometer ASL separation). Blue: river or channel. Brown: road.

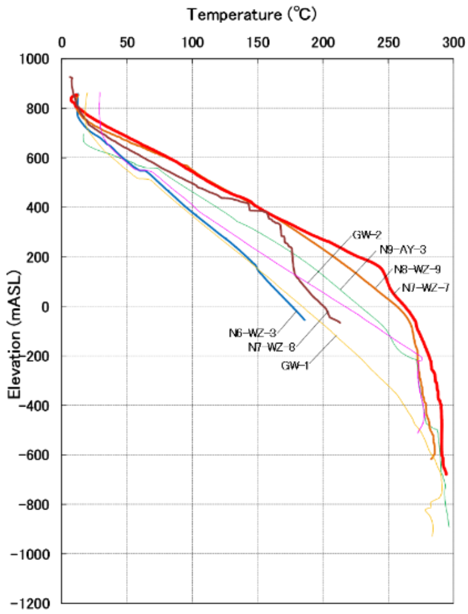

Figure 2: Stable temperature profiles in representative wells in the Wasabizawa geothermal field.

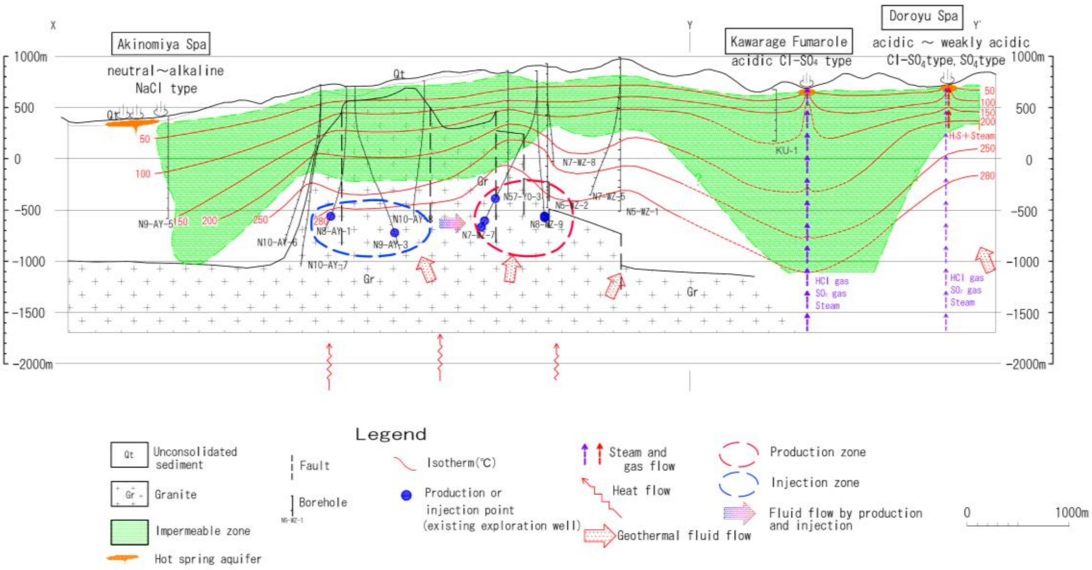

Figure 3: Conceptual model of the Wasabizawa field from south-west (left) to north-east (right). Inferred temperature distribution is shown by solid red lines. Green shaded area shows a cap rock layer and western and eastern impermeable zones. The reservoir is hosted by naturally-fractured granitic rocks. Conceptualized fluid flow pathways are indicated by arrows. Planned production and reinjection zones are shown by red and blue thick dashed circles respectively.

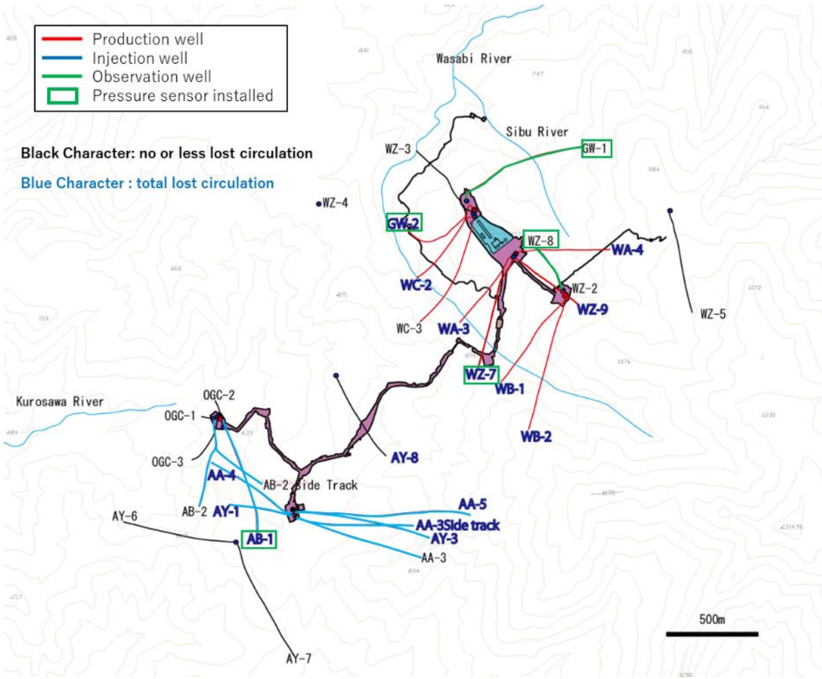

Figure 4: Locations of newly drilled wells and exploration wells in production and injection wellfields. WA, WB, WC, AA and AB series wells are newly drilled wells during construction of the power station. Others are exploratory wells including five wells which will be converted to production (WZ-7, WZ-9 and GW-2) and injection (AY-1 and 3) wells. Red well trace: production wells. Blue well trace: injection wells. Green text box: pressure observation well during interference tests

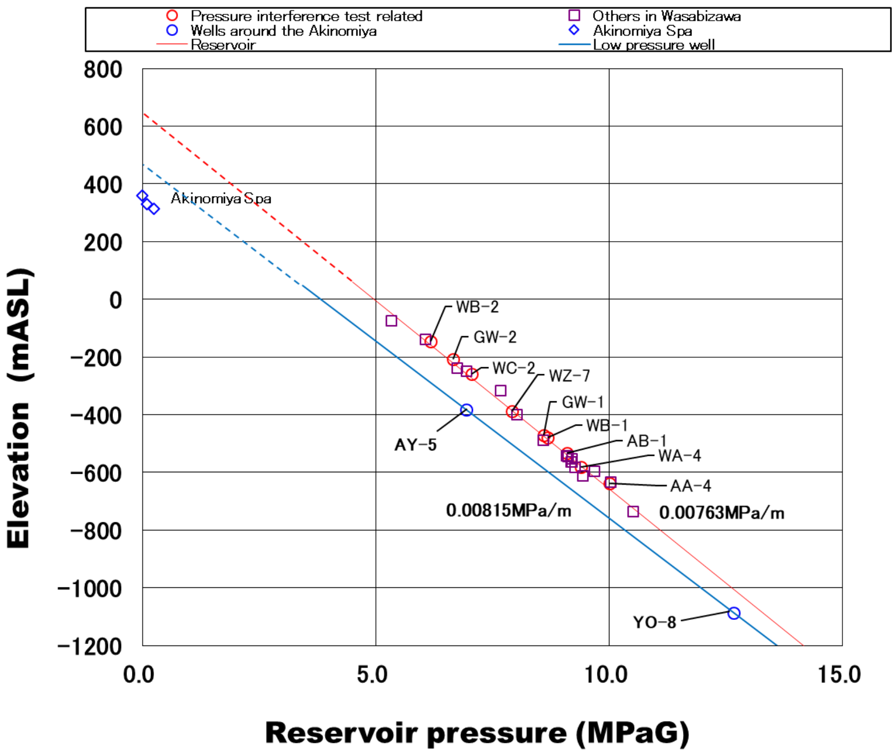

Figure 5: Measured downhole feedpoint pressures in wells versus feedpoint elevation. Straight lines show least-squares fits to high pressure and low pressure wells respectively. Feedpoint pressures of newly drilled production and injection wells as well as those of pressure observation wells during interference tests are all fit by the (high pressure) reservoir pressure gradient line. The Akinomiya hot spring area to the south-west of the field where the low pressure wells are located has natural ground surface springs and shallow wells, and data from representative springs are shown in the figure.

2. PRESSURE TRANSIENT TESTS

To delineate the permeability structure for the area quantitatively, numerous pressure transient tests were performed during short term production and injection tests for newly drilled wells.

2.1 Single Well Tests

Single well pressure transient tests (fall off tests and build up tests) were conducted to evaluate formation and well parameters (i.e. transmissivity (kh), skin factor (s) etc.) for newly drilled wells. After drilling a new well, PTS (Pressure, Temperature and Spinner) loggings were performed under both static and flowing conditions to delineate locations of feedpoint(s) in the well. Then, step rates water injection test was performed by setting P & T gauges at the main feedpoint depth, and pressure transient data including pressure fall off data after shut-in were recorded. For production wells, short term production tests with a duration of only a week or so were also performed to confirm well productivity and to obtain well characteristics (i.e. Flowrate vs. Wellhead pressure). For production tests, PTS loggings were also performed under both static and flowing conditions, and pressure buildup tests were performed by setting PT gauges at the main feed point depth and shutting-in the well. These pressure transient data were analyzed by conventional Horner plot as well as by using DIAGNS (McLaughlin et al. (1995)) which uses an automated nonlinear regression algorithm to produce the best match between the computed and measured pressures and to determine the unknown parameters in the mathematical model like permeability-thickness kh, storage parameter ϕch and so on. The analyses were all performed using the finite cylindrical-source model.

Table 1 summarizes these results for production and injection wells of the power plant including previously drilled exploration wells which were converted to production (GW-2, WZ-7 and 9) and injection wells (AY-1 and 3). The formation parameters for NEDO survey wells are from NEDO reports; these data were analyzed by conventional type curve matching. Newly drilled wells AB-2 (with a sidetracks) and WC-3 did not penetrate permeable fractures, and are therefore excluded from Table 1. Pressure transient data from injection tests of WA-4 and WB-1 were unanalyzable because these data were severely affected by change in temperature in water column in the well due to ill-positioning of the pressure gauge in the well. Data from buildup test of WA-3 was also unanalyzable, because the well had two phase feed condition at all feedpoints during production, and the buildup data was inappropriate for analysis with analytical solutions. While short term production tests of GW-2 and WC-2 were conducted to obtain wellhead flow characteristics, pressure buildup tests were not conducted for these wells due to unsuitable wellbore conditions after workover jobs. Productivity and injectivity indices calculated by using the difference between feedpoint pressures under static and flowing conditions are also shown in Table 1.

Transmissivities inferred by using DIAGNS are comparable with those inferred by Horner plot on the whole as shown in Table 1, and an extensive heterogeneity of permeability was observed among newly drilled 11 production and injection wells. Table 1 shows that wells WA-4, WB-1 and WC-2 penetrated relatively large fractures with high permeability and are good producers. Injection well AB-1 has also relatively high transmissivity. Other newly drilled wells except two wells (AB-2 and WC-3) have a modest transmissivity of 2-7 Darcy-m, about the same as the inferred values for NEDO survey wells.

Table 2: Results of single well tests for newly drilled wells and exploratory wells.

Well		Feed point (mASL)	Test	Transmissivity* kh (darcy-m)	Storage parameter φch (m/Pa)	Skin factor S (-)	Injectivity or Productivity index II or PI (kg/sec/bar)	Remarks
Production Well (Newly drilled)	WA-3	-543	Falloff	6.7 (2.4)	2.0×10^{-9}	0.4	1.2	
			Buildup					Unanalyzable
	WA-4	-580	Falloff					Unanalyzable
			Buildup	30 (14)	5.4×10^{-8}	20	6.6	
	WB-1	-480	Falloff					Unanalyzable
			Buildup	26 (12)	1.4×10^{-7}	-4.8	6.8	
	WB-2	-146	Falloff	2.3 (2.8)	3.2×10^{-7}	5.7	1.1	
			Buildup	2.2 (1.8)	3.7×10^{-7}	7.6	1.2	
	WC-2	-258	Falloff	43 (39)	5.3×10^{-9}	-6.3	43	
			Buildup					Not conducted
Production Well (Converted from exploration well)	WZ-7	-388	Falloff	5.4	1.3×10^{-11}	5.4	1.2	NEDO's survey
			Buildup	1.0	8.8×10^{-7}	1.0	0.4	NEDO's survey
	WZ-9	-581	Falloff					Not conducted
			Buildup	5.0	4.4×10^{-8}	20	0.8	NEDO's survey
	GW-2	-207	Falloff	8.8	5.4×10^{-3}	2.5	7.8	
			Buildup					Not conducted
Injection Well (Newly drilled)	AA-3a	-707	Falloff	2.3 (3.0)	2.1×10^{-7}	15	1.5	
	AA-4	-639	Falloff	5.0 (4.1)	3.5×10^{-8}	2.5	1.2	
	AA-5	-487	Falloff	2.3 (1.9)	1.0×10^{-6}	2.6	1.2	
	AB-1	-533	Falloff	17 (24)	1.0×10^{-7}	9.6	2.7	
Injection Well (Convertd from exploration well)	AY-1	-563	Falloff	1.2	2.6×10^{-7}	-5.0	2.4	NEDO's survey
	AY-3	-725	Falloff	4.8 (1.5)	2.0×10^{-9}	-2.9	2.4	

*Transmissivity values in parentheses are inferred by Horner plots

2.2 Pressure Interference Tests

YGP conducted short term production tests for newly drilled production wells. These tests were carried out for each production well pad; WA, WB and WC. Production durations for these tests were limited to a week or so per well due to tight schedule of construction works. This field is located in a heavy snowfall area, and the time period for construction works in the field was limited to about 7 or 8 months a year. In 2017, capillary tube type pressure sensors were installed in five shut-in wells (WZ-7, WZ-8, GW-1, GW-2 and AB-1; see Figure 4) to observe pressure interference in the reservoir due to production tests of wells WB-1 and 2. During the short term production tests of these wells, separated brine was injected into a production well WA-4. Figure 6 shows the feedpoint locations of all the production, injection and observation boreholes involved in these pressure interference tests. Figure 7 shows changes in pressure in observation wells as well as flow conditions of active wells. Pressure interference due to the production tests were observed apparently in many wells except in well AB-1 located far away from production well. In addition to pressure response to the production tests, changes in pressure due to injection tests and total lost circulation in drilling of other wells were also observed. In some wells (AB-1 etc.), poor quality data with oscillatory pressure changes were obtained due to effects of ambient temperature change on the surface quartz pressure gauge. Pressure interference analyses were conducted to evaluate permeability structure of the reservoir quantitatively by using DIAGNS (McLaughlin et al. (1995)). The in situ temperature of reservoir water and viscosity is assumed to be 280°C and 0.9×10^{-4} Pa-s, respectively. An initial pressure was assigned from the results of single well tests or pressure value obtained before interference test started. The analyses were all performed using the line-source model using distances between feedpoints of observation and active wells.

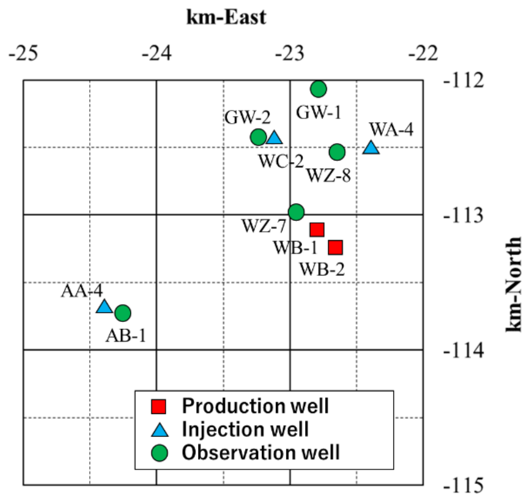

Well	Usage(**during pressure transient tests**)	Feed point coordinates		Feed point Depth (mASL)
		m (North)	m (East)	
WZ-7	Observation	-112983	-22949	-388
WZ-8	Observation	-112531	-22648	-24
GW-1	Observation	-112043	-22797	-470
GW-2	Observation	-112453	-23219	-207
WA-4	Injection	-112510	-22387	-580
WB-1	Production	-113121	-22791	-480
WB-2	Production	-113253	-22660	-146
WC-2	Injection	-112449	-23129	-258
AA-4	Injection	-113688	-24388	-639
AB-1	Observation	-113724	-24263	-533

Figure 6: Horizontal feedpoint locations of wells related to the pressure interference tests. In well AB-1, no pressure interference from production tests was observed, and the pressure response to injection test of nearby AA-4 was observed.

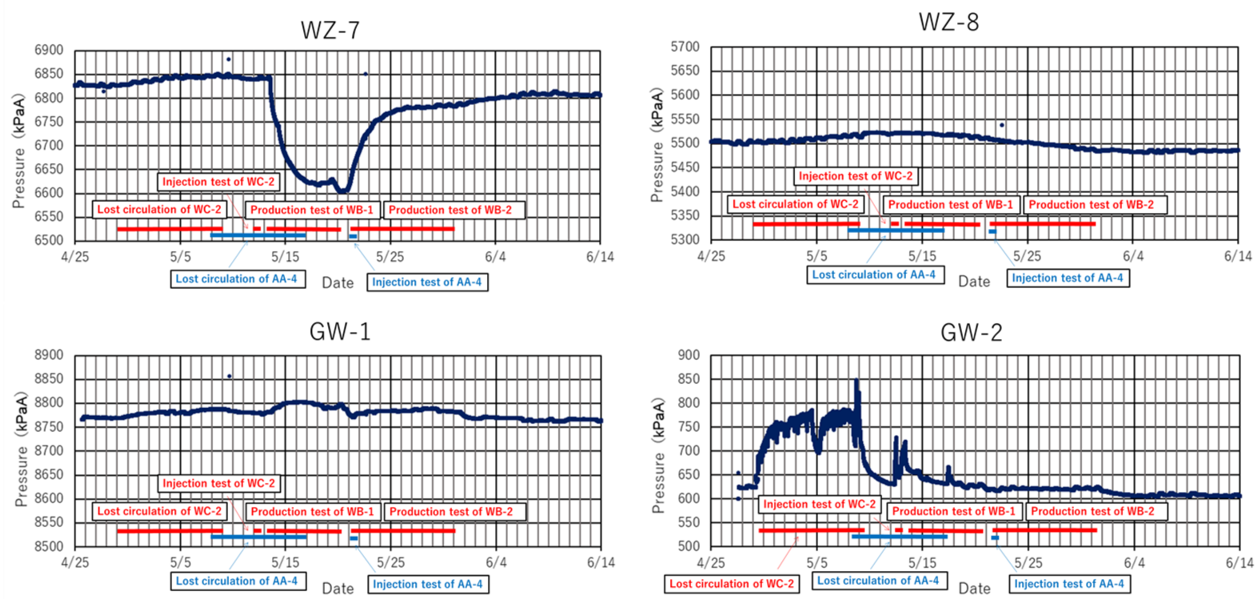

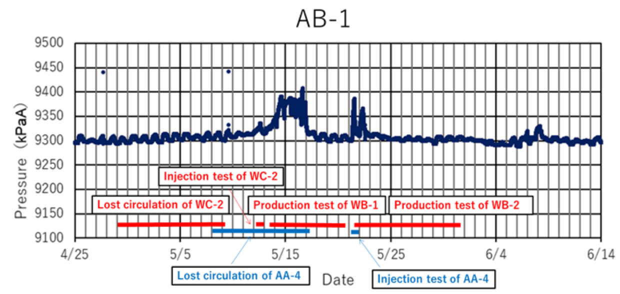

Well test and lost circulation period

- <u>Production test of WB-1 (Injection well: WA-4)</u>
  2017/5/13 13:30～2017/5/20 20:00
- <u>Production test of WB-2 (Injection well: WA-4)</u>
  2017/5/21 10:00～2017/5/31 13:20
- <u>Total lost circulation of WC-2</u>
  2017/4/29 6:00～2017/5/8 11:00
- <u>Injection test of WC-2</u>
  2017/5/11 9:05～2017/5/11 12:35
- <u>Injection test of AA-4</u>
  2017/5/21 9:00～2017/5/21 13:30

Figure 7: Pressure changes in observation wells. Pressure changes due to well tests and total lost circulation during drilling of WC-2 and AA-4 were observed as well as pressure interference from production tests of WB well pad.

<u>2.2.1 WZ-7</u>

a) Production test of WB-1

WB-1 is a new production well drilled in 2016 and production test was conducted for 7 days in 2017. WB-1 has high productivity. Figure 8 shows flow histories for all the active production and injection wells during production tests of WB pad wells. WA-4 was used as injection well in the test. During the test, drawdown of reservoir pressure due to production from WB-1 was observed in WZ-7. We assumed that injection into WA-4 also affected on the pressure response in the analysis, taking account of the distance between feedpoints of WZ-7 and WA-4; those are located less than 1 km away from each other. Figure 9 shows measured and computed pressures. Pressure data after 90 hours were not used for analysis because data quality was bad (oscillations due to ambient temperature change).

Active wells: Production well: WB-1
Injection well: WA-4
The final model parameters are:
kh = 11.7 Darcy-m
$\phi ch = 4.1 \times 10^{-8}$ m/Pa

Fracture network among WZ-7, WB-1 and WA-4 has modest transmissivity of 11.7 Darcy-m.

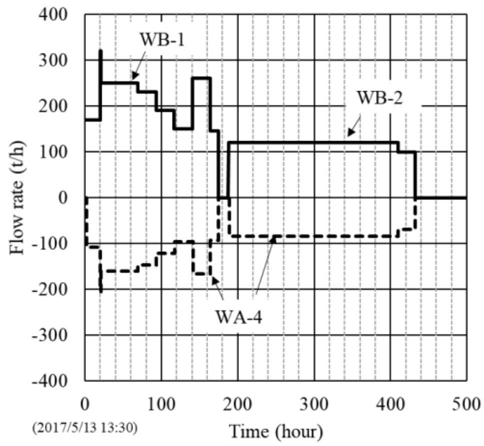

Figure 8: Flow histories for production tests of WB pad wells. Negative value indicates injection.

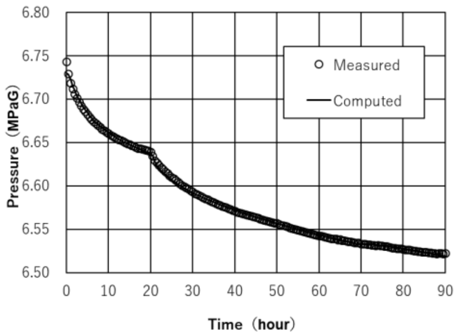

Figure 9: Comparison of measured pressures in WZ-7 with computed response due to production from WB-1 and injection into WA-4. Pressure data interval is 30 minutes.

b) Production test of WB-1 and WB-2
WB-2 is a new production well drilled in 2016 and production test was conducted for 10 days just after production test of WB-1. During these tests, drawdown of pressure was observed. After these tests, buildup of reservoir pressure was observed in WZ-7. Pressure buildup data after shut-in of WB-2 was used in the analysis. This pressure change was relatively small and effect of ambient temperature change were significant. Pressure data at around 8:00AM and 8:00PM for each day were used in the analysis. Figure 10 shows measured pressures and computed pressure response.

Active wells: Production well: WB-1, WB-2
Injection well: WA-4
The final model parameters are:
kh = 7.2 Darcy-m
$\phi ch = 3.4 \times 10^{-7}$ m/Pa

Transmissivity obtained in this analysis is lower than that obtained from the production test of WB-1 alone. This is consistent with the fact that transmissivity obtained by single well test of WB-2 has a relatively low value of 2.2 Darcy-m (see Table 1). The inferred value for the storage parameter ϕch is fairly high. The large storage parameter shows that a two phase zone exists near the feedpoint of WB-2 which has a relatively high elevation (see Figure 5).

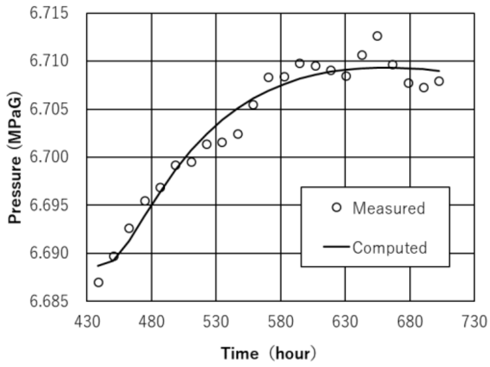

Figure 10: Comparison of measured pressures in WZ-7 with computed response after stoppage of production from WB-1 and WB-2. Pressure data interval is 12 hours.

c) Lost circulation of WC-2
During drilling of WC-2, total lost circulation (1200L/min) occurred. Minor increase in reservoir pressure was observed in WZ-7 in response to the lost circulation. Figure 11 shows measured pressures and computed pressure response. Measured pressure data were sampled in the same way as for analysis b).

Active well: Injection well: WC-2 (total lost circulation)
The final model parameters are:

kh = 9.1 Darcy-m

$\phi ch = 1.3\times10^{-7}$ m/Pa

Transmissivity between WZ-7 and WC-2 is bracketed by the transmissivities obtained from single well test for WZ-7 and WC-2. The inferred value for the storage parameter ϕch is fairly high.

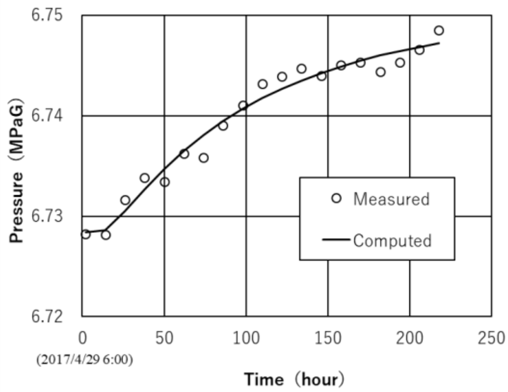

Figure 11: Comparison of measured pressures in WZ-7 with computed response due to lost circulation in WC-2. Pressure data interval is 12 hours.

2.2.2 GW-1

GW-1 is an exploratory well with little transmissivity and was converted to an observation well. Despite low transmissivity of GW-1, pressure interference was observed. During production test in WB pad, increase in reservoir pressure due to reinjection into WA-4 was observed in GW-1. We assumed that production from wells WB-1 and 2 also affected on the pressure response in the analysis. Figure 12 shows measured pressures and computed pressure response.

Active wells: Production well: WB-1, WB-2
Injection well: WA-4
The final model parameters are:

kh = 8.9 Darcy-m

$\phi ch = 3.2 \times 10^{-8}$ m/Pa

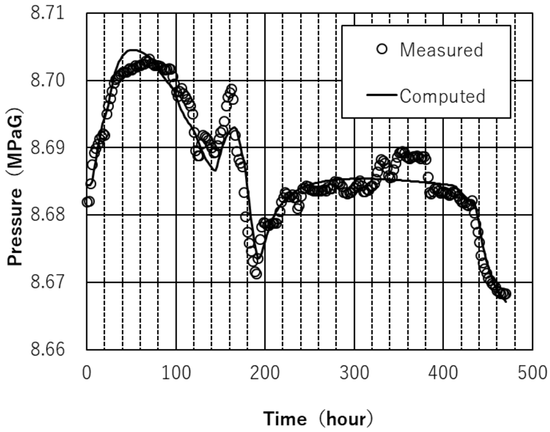

Figure 12: Comparison of measured pressures in GW-1 with computed response due to production test in WB pad. Measured pressure data interval is 120 minutes.

2.2.3 GW-2

a) Production test of WB-1 and WB-2

After production test in WB pad, pressure drawdown due to stoppage of injection into WA-4 was observed in GW-2. Unlike the case of GW-1, increase in reservoir pressure due to injection into WA-4 was not notable. We assumed that all the active wells affected on the pressure response. Figure 13 shows measured pressures and computed pressure response. Measured pressure data were edited in same way as for analysis b) for well WZ-7.

Active wells: Production well: WB-1, WB-2
Injection well: WA-4
The final model parameters are:
kh = 2.6 Darcy-m
$\phi ch = 2.1\times 10^{-8}$ m/Pa

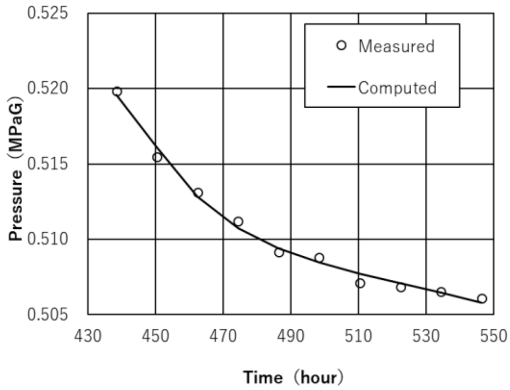

Figure 13: Comparison of measured pressures in GW-2 with computed response due to injection test of WC-2. Pressure data interval is 12 hours.

b) Injection test of WC-2

WC-2 is a new production well drilled in 2017 and a short-term injection test was conducted after drilling. Figure 14 shows flow history for this test. During this test, an increase in pressure was observed in GW-2. Distance between feedpoints of WC-2 and GW-2 is very small. Figure 15 shows measured pressures and computed pressure response.

Active well: Injection well: WC-2
Observation well: GW-2
The final model parameters are:
kh = 16.7 Darcy-m
$\phi ch = 1.0 \times 10^{-8}$ m/Pa

Transmissivity between WC-2 and GW-2 is relatively high and is bracketed by the transmissivities for the two wells listed in Table 1.

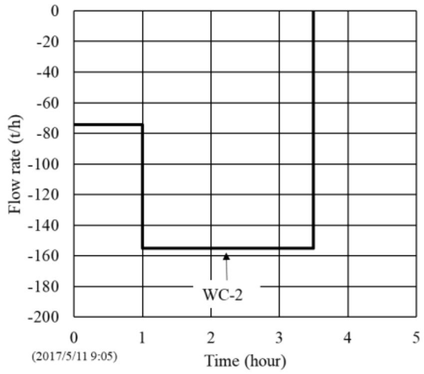

Figure 14: Flow history for injection test of WC-2. Negative value indicates injection.

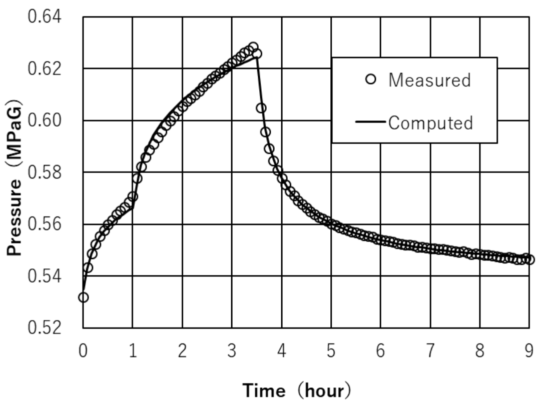

Figure 15: Comparison of measured pressures in GW-2 with computed response due to injection test of WC-2. Pressure data interval is 5 minutes.

2.2.4 AB-1

AA-4 is a new injection well drilled in 2017 and a short term injection test was conducted for 4 hours. Figure 16 shows the flow history. During this test, increase in reservoir pressure was observed in AB-1. AB-1 is also a new injection well which has high transmissivity (Table 1). Figure 17 shows measured pressures and computed pressure response.

Active well: Injection well: AA-4
Observation well: AB-1
The final model parameters are:

kh = 10.2 Darcy-m

$\phi ch = 6.1 \times 10^{-9}$ m/Pa

Distance between feedpoints of AA-4 and AB-1 is very small. Analysis of the pressure interference data indicates that wells AA-4 and AB-1 are connected by a modest transmissivity (kh ~ 10 Darcy-m) and a low storativity ($\phi ch \sim 6 \times 10^{-9}$ m/Pa) fracture zone. The inferred transmissivity value does not represent formation transmissivity at the reservoir length scale.

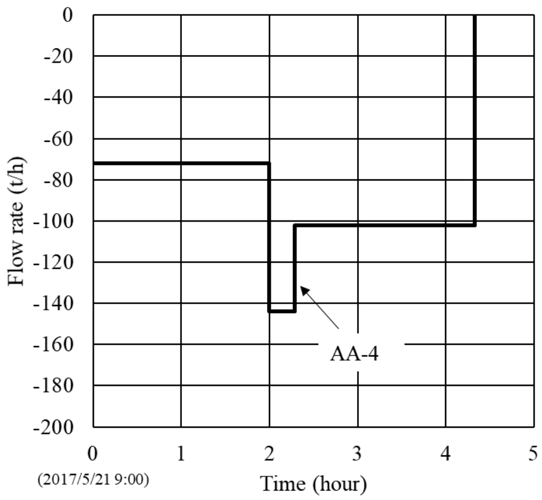

Figure 16: Flow history of injection test of AA-4. Negative value indicates injection.

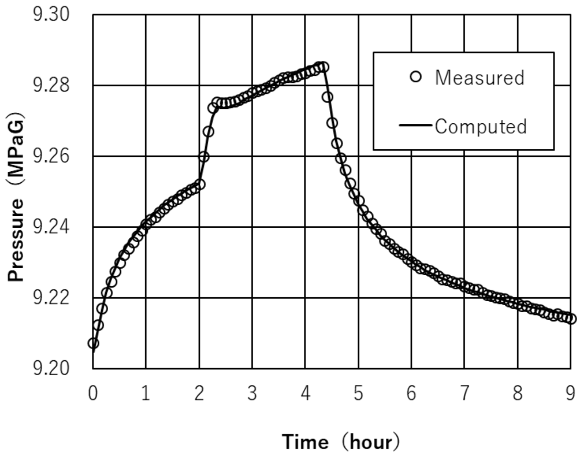

Figure 17: Comparison of measured pressures in AB-1 with computed response due to injection to AA-4. Pressure data interval is 5 minutes.

2.3 Synthesis of the Pressure Transient Analyses

Figure 18 shows a summary of the analyses of single well pressure transient tests and pressure interference tests. Targeting the fault zones inferred from geophysical surveys, a total of 11 production and injection wells, in addition to five existing exploration wells which will be converted to production and injection wells, were drilled during construction of the power station, and an extensive heterogeneity of fracture distribution in the granitic basement rock was observed. For example, along the inferred fault zone striking NW-SE, WC-2 located to the north and WB-1 (and WA-3) located to the south penetrated highly permeable fracture zones, and there is no permeable fractured area (along well trace of WC-3) between WC-2 and WB-1. None the less, analyses of pressure interference data indicate that a fracture network is present in the granitic basement rock, and the reservoir has a modest transmissivity of 3-17 Darcy-m. Reservoir temperature and pressure profiles suggest that two phase regions (steam cap) may exist at the top of the reservoir just below the cap rock in eastern part of the field where depth of reservoir top is relatively shallow. Relatively large value for the storage parameter ϕch ($1\text{-}3 \times 10^{-7}$ m/Pa) obtained by pressure interference analysis in production wellfield might also suggest that steam cap exists at the top of the reservoir and affects the pressure transient response.

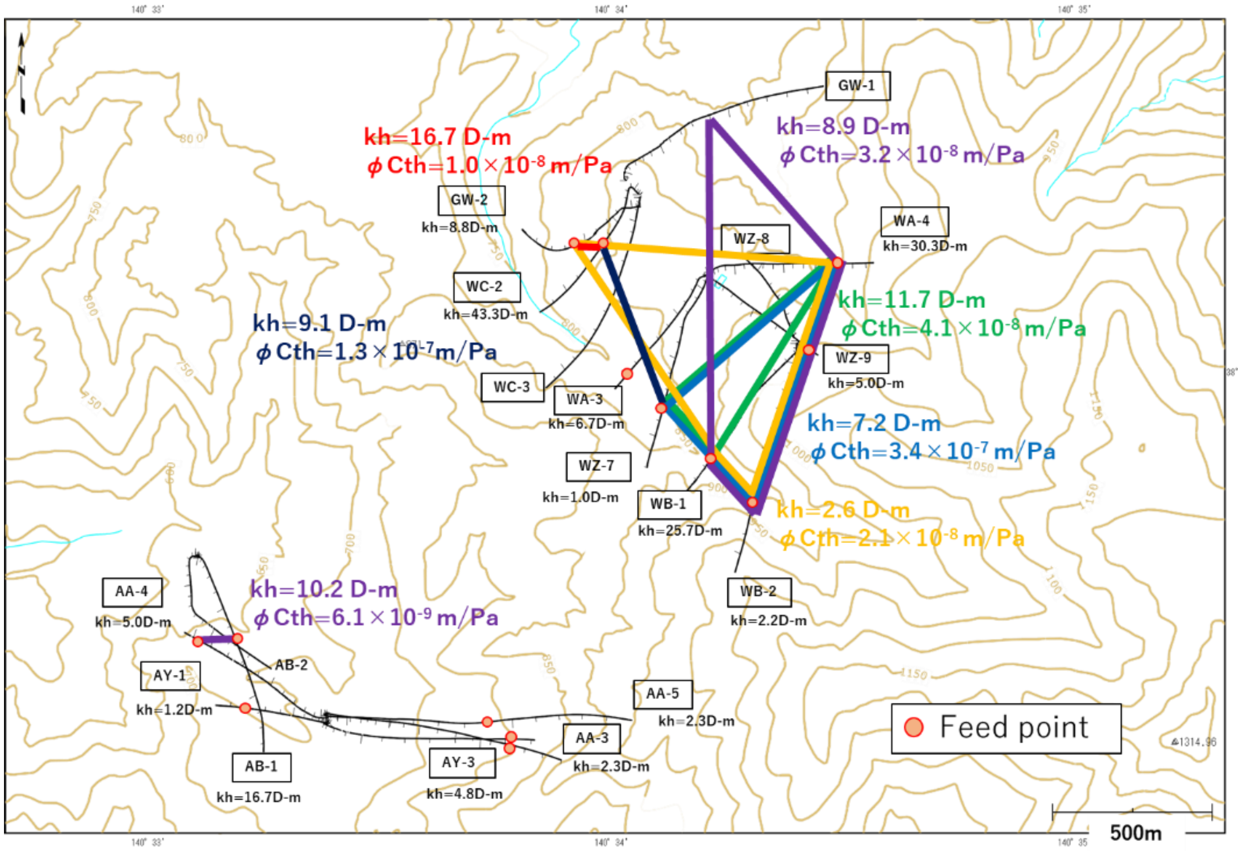

Figure 18: Summary of pressure interference tests. Thick straight lines of different color show the connections between observation and active wells for each pressure interference analysis. Transmissivity inferred from single well test are shown under well name box.

3. CONCLUDING REMARKS

To delineate the permeability structure for the Wasabizawa geothermal field, numerous pressure transient tests were performed. Pressure interference tests were invaluable for characterizing the permeability structure of the area. Analyses of pressure interference data indicate that the reservoir has a modest transmissivity of 3-17 Darcy-m. Relatively large value for the storage parameter ϕch (1-3 × 10^{-7} m/Pa) indicates that a two-phase region (steam cap) exists just below the cap rock where the reservoir top is relatively shallow, and it supports the present conceptual model.

4. ACKNOWLEDGEMENTS

The authors wish to thank the management of J-Power, MMC, MGC and YGP for the permission to publish this paper.

REFERENCES

McLaughlin, K.L., Baker, T.G., Owusu, L.A. and Garg, S.K.; DIAGNS: An interactive workstation-based system for well test data diagnostics and inversion, *Proceedings*, World Geothermal Congress, Florence, (1995), 2941-2944

Nakanishi, S., Todaka, N., Tezuka, S., Akasaka, C., Sasaki, K., Kitao, K., Kaneko, T. and Ajima S.: A conceptual model of the Wasabizawa geothermal field, Akita prefecture, Japan, *Proceedings*, World Geothermal Congress 2020, Reykjavik (2020).